Monitoring nonadiabatic dynamics in molecules by ultrafast X-Ray diffraction

Markus Kowalewski[1*], *Kochise* Bennett[2], *Shaul* Mukamel[3]
[1]*Department of Physics, Stockholm University, AlbaNova University Center, 10691 Stockholm, Sweden.*
[2]*Department of Chemistry, University of California, Berkeley, California 94720, USA*
[3]*Chemistry Department, Department of Physics and Astronomy, University of California, Irvine, California 92697-2025, USA*

Abstract: We theoretically examine time-resolved diffraction from molecules which undergo non-adiabatic dynamics and identify contributions from inelastic scattering that indicate the presence of an avoided crossing and the corresponding nuclear configuration.

1. Introduction

X-ray diffraction has long been used to analyze the structure of crystals. Time-resolved X-ray diffraction can track the structural changes that characterize phase transitions and chemical reactions and has been actively pursued to create movies of elementary molecular events. Free electron lasers allow for extremely bright and ultrafast X-ray pulses and make it possible to measure diffraction in low density samples. In addition, their femtosecond timescale opens up the possibility of tracking sub-femtosecond electronic dynamics.

In this contribution, we show how time-resolved X-ray diffraction may be used to obtain real-time stroboscopic snapshots of nonadiabatic molecular dynamics. When a photoexcited molecule passes through a conical intersections or an avoided crossing a short-lived electronic coherence is created, which may be spectroscopically detected [1,2] by X-rays. We examine the elastic and inelastic contributions to the diffraction pattern that stem from the coupled nonadiabatic electronic+nuclear dynamics in the vicinity of an avoided crossing. Time-resolved scattering from photoexcited molecules in the gas phase is given by an incoherent sum of single-molecule contributions, contains elastic and inelastic terms, and may depend on electronic coherence. We identify five distinct contributions to the signal and study their relative intensity and time-resolved diffraction pattern. Contributions from electronic coherences, which are created in the avoided crossing region are of particular interest. The underlying molecular quantities are the transition charge densities between electronic states.

2. Time resolved diffraction in gas phase

The off-resonant scattering signal in the gas phase can be expressed through a correlation function of the charge density operators $\hat{\sigma}$ [3,4]:

$$S(\mathbf{q},t) = N\int \mathrm{d}t |E_p(t)|^2 \langle \hat{\sigma}^\dagger(\mathbf{q},t)\hat{\sigma}(\mathbf{q},t)\rangle \tag{1}$$

here $E_p(t)$ is the temporal envelope of the X-ray probe pulse, $\langle \ldots \rangle$ stands for expectation value over the nuclear and electronic states, $\hat{\sigma}(\mathbf{q},t)$ is the spatial Fourier transform of the charge-density operator, and N the number of molecules. Expanding the single molecule diffraction signal in electronic eigenstates yields an expression with five different contributions:

$$\begin{aligned}\langle \hat{\sigma}^\dagger(\mathbf{q},t)\hat{\sigma}(\mathbf{q},t)\rangle = \Big\{ &\underbrace{\rho_{ee}(t)\langle\chi_e(t)|\hat{\sigma}^\dagger_{ee}\hat{\sigma}_{ee}|\chi_e(t)\rangle}_{\text{(i)}} + \underbrace{\rho_{gg}(t)\langle\chi_g(t)|\hat{\sigma}^\dagger_{gg}\hat{\sigma}_{gg}|\chi_g(t)\rangle}_{\text{(ii)}} \\ &+ \underbrace{\rho_{ee}(t)\langle\chi_e(t)|\hat{\sigma}^\dagger_{eg}\hat{\sigma}_{ge}|\chi_e(t)\rangle}_{\text{(iii)}} + \underbrace{\rho_{gg}(t)\langle\chi_g(t)|\hat{\sigma}^\dagger_{ge}\hat{\sigma}_{eg}|\chi_g(t)\rangle}_{\text{(iv)}} \\ &+ \underbrace{2\Re\left[\rho_{eg}(t)\langle\chi_e(t)|\hat{\sigma}^\dagger_{ee}\hat{\sigma}_{eg}|\chi_g(t)\rangle + \rho_{eg}(t)\langle\chi_e(t)|\hat{\sigma}^\dagger_{eg}\hat{\sigma}_{gg}|\chi_g(t)\rangle\right]}_{\text{(v)}} \Big\}\end{aligned} \tag{2}$$

where the electronic populations and coherences are given by the diagonal and off-diagonal elements of the density matrix $\rho_{ij}(t)$ respectively and we have defined the electronic-state matrix elements of the charge-density operator $\hat{\sigma}_{ij} \equiv \langle\phi_i|\hat{\sigma}(\mathbf{q})|\phi_j\rangle$ in the basis of the electronic states $\phi_{i/j}$. $\chi_{g/e}(R,t)$ are the nuclear wave functions on the respective electronic surfaces. The corresponding loop diagrams for term (i) through (v) are shown in Fig. 1.

The first two terms on the right-hand side of Eq. (2) (i) and (ii) represent the elastic diffraction from states e and g respectively, which encode the time evolution of the nuclear wave packets in each of the two electronic states. The next two terms, (iii) and (iv), represent the inelastic scattering from the electronic ground and excited state populations respectively. The last term (v) is due to scattering off electronic coherences between $|g\rangle$ and $|e\rangle$. This term contributes to the diffraction image, when a super position of states g and e is present.

Corresponding author: markus.kowalewksi@fysik.su.se

Note that Eq. 1 describes the diffraction of a sample in gas phase (i.e. no long range order). This diffraction image is fundamentally different from diffraction of a crystalline sample. The single particle signal lacks not only Bragg peaks buts also scales linear with the number of particles (vs. quadratic) and does not contain heterodyne interference between particles. The single particle diffraction image is determined by products of charge density operators, $\langle \sigma^+ \sigma \rangle$, while in the crystalline case the charge density can be factorized: $\langle \sigma \rangle^2$.

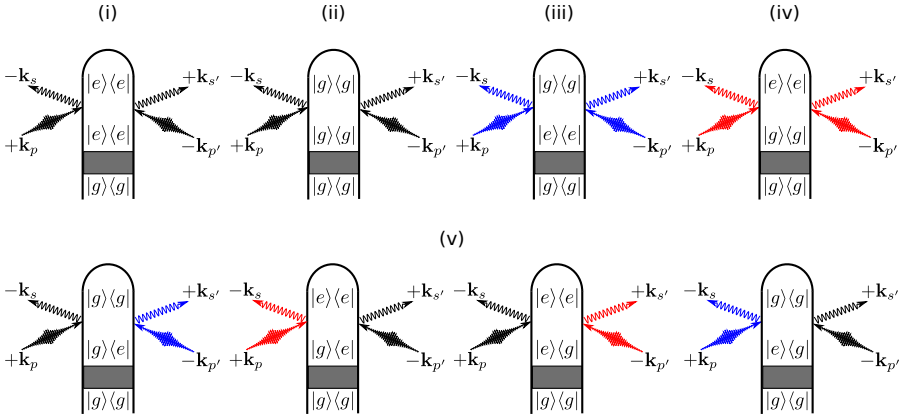

Fig 1. Loop diagrams for single-molecule X-ray scattering processes as given by Eq. (2). The shaded area represents preparation with a pump-pulse. Diagrams for elastic scattering from e and g is shown in (i) and (ii) respectively, while the diagrams for inelastic scattering from e and g are displayed in (iii) and (iv). The bottom row (v) represents all diagrams involving to electronic coherences. Elastic scattering processes come with $\hat{\sigma}_{gg}$ or $\hat{\sigma}_{ee}$ and are denoted by black field arrows. Inelastic processes in which the molecule gains (Stokes) or loses (anti-Stokes) energy to the field come with $\hat{\sigma}_{ge}$ or $\hat{\sigma}_{eg}$ depending whether the action is on the ket or bra and are denoted with red and blue field arrows to indicate the field's spectral shift due to the particular diagram. Figures reused from [3] https://creativecommons.org/licenses/by/4.0/

3. Results

To demonstrate the influences of the coherence contribution (v) we use the avoided crossing dynamics of NaF as an example. The electronic structure of NaF was calculated at the CAS(8/9)/MRCI/aug-cc-pVTZ level of theory. The wave packet dynamics of the nuclei following a 10 fs UV pump-pulse was performed numerically on a spatial grid including the covalent $X^1\Sigma$ (g), and the ionic $A^1\Sigma$ (e) state potential energy curves. The dynamics is probed after a delay T with a 2.5 fs, hard X-ray probe pulse and the diffraction image is calculated according to Eq. 1.

Figure 2 (left panel) shows the potential energy curves involved in the dynamics. The avoided crossing at 8.3 Å causes the nuclear wave packet to branch via the non-adiabatic couplings. Figure 2 (right panel) shows the time evolution of the population of the $A^1\Sigma$ state. At 220 fs the nuclear reaches the avoided crossing and an electronic coherence between the $X^1\Sigma$ and $A^1\Sigma$ is created (blue curve, dip at 220 fs).

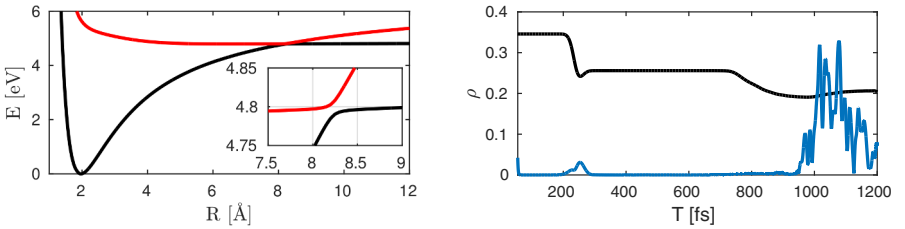

Fig 2. Right panel: Time evolution of the excited-state population ($A^1\Sigma$, black) and the magnitude of the coherence $|\rho_{eg}|$ (blue). The coherence at 220 fs is created by the outward wave packet passing through the avoided crossing, while the strong coherence around 1100 fs corresponds to the wave packet return to the Franck-Condon region. Left panel: Potential energy curves of NaF (black $X^1\Sigma$, red $A^1\Sigma$). The wave packet branches at the avoided crossing at 8.3 Å. Figures reused from [3] https://creativecommons.org/licenses/by/4.0/

In Figs. 3(a) and (b) the contributions from term (i) to diffraction image are shown in reciprocal space and real space respectively. This corresponds to diffraction signal of the excited state charge density. The inverse Fourier transform of the diffraction image in momentum space, reveals wave packet motion (Fig. 3(b)). Since the charge density is dominated by a sharply peaked density of the core electrons, Fig. 3(b) can be qualitatively interpreted as the shape of the nuclear wave packet, $|\chi(R,t)|^2$. The back-and-forth oscillation on the $A^1\Sigma$ state potential energy surface is clearly visible in this component of the real-space diffraction image.

In Figs. 3(c) and (d) the contributions from term (v) to the diffraction image are shown in reciprocal space and

real space respectively. This part corresponds to the inelastic coherence contributions. The charge density matrix elements responsible for this part of the diffraction image are a convolution of charge density and transition charge density matrix elements, $\sigma_{ii}\sigma_{ij}$. Furthermore, they carry the electronic coherence, ρ_{ij}, as pre-factor. As can be seen in Fig. 3(c), a clear oscillatory signature at ≈ 220 fs appears in the diffraction pattern – the point in time when the nuclear wave packet passes over the avoided crossing. The real space diffraction image in Fig. 3(d) places the signature at ≈ 8 Å, where the avoided crossing is located.

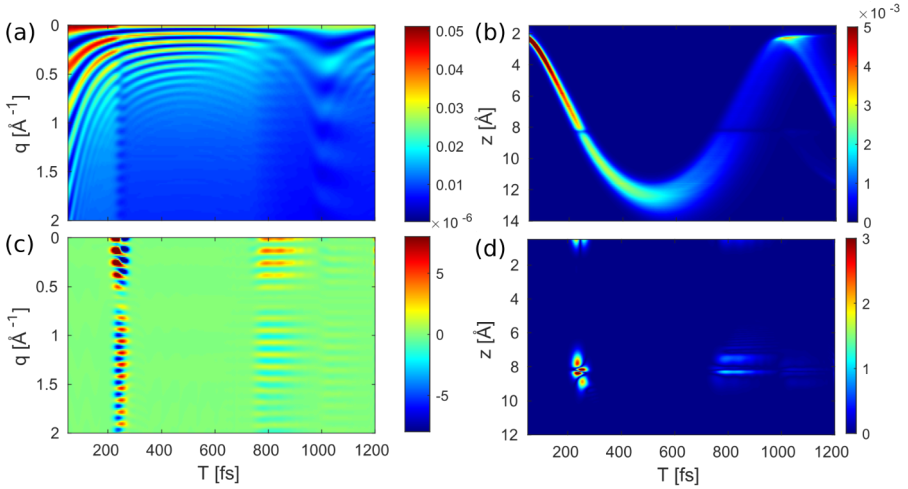

Fig 3. Selected diffraction images calculated by Eqs. 1 and 2. (a) Contribution from the exited state $A^1\Sigma$ (i). (b) Inverse Fourier transform of (a). (c) Inelastic contribution from the electronic coherence (v). (d) Fourier transform of (c).

4. Conclusions

We have shown that the gas phase diffraction signal contains not only elastic contributions from the charge densities of the electronic states involved but also inelastic scattering contributions. Those inelastic contributions depend on electronic coherences and create signatures in the diffraction image. The coherence contributions do not merely indicate that a coherence has been created but also reveal spatial information about the nuclear configuration involved. The next step is the investigation of electronic coherences created around conical intersections in polyatomic molecules.

5. References

[1] M. Kowalewski, K. Bennett, K. E. Dorfman, and S. Mukamel, "Catching conical intersections in the act: Monitoring transient electronic coherences by attosecond stimulated X-Ray raman signals", Phys. Rev. Lett. **115**, 193003 (2015).

[2] M. Kowalewski, K. Bennett, J. R. Rouxel, and S. Mukamel, "Monitoring nonadiabatic electron-nuclear dynamics in molecules by attosecond streaking of photoelectrons", Phys. Rev. Lett. **117**, 043201 (2016)

[3] M. Kowalewski, K. Bennett, and S. Mukamel, "Monitoring nonadiabatic avoided crossing dynamics in molecules by ultrafast X-ray diffraction", Struct. Dynam. **4**, 054101 (2017)

[4] M. Kowalewski, K. Bennett, J. R. Rouxel, and S. Mukamel, "Monitoring molecular nonadiabatic dynamics with femtosecond X-ray diffraction", Proc. Natl. Acad. Sci. USA **115**, 6538 (2018).